Evolution of the alkyl-chain dynamics in monolayer-protected gold clusters

R. Mukhopadhyay,[1,*] S. Mitra,[1] M. Johnson,[2] V. R. Rajeev Kumar,[3] and T. Pradeep[3,†]

[1]*Solid State Physics Division, Bhabha Atomic Research Centre, Mumbai 400 085, India*

[2]*Institute Lau-Langevin, BP156, F-38042, Grenoble, Cedex 9, France*

[3]*DST Unit on Nanoscience, Department of Chemistry and Sophisticated Analytical Instrument Facility,*
Indian Institute of Technology Madras, Chennai 600 036, India

Alkyl-chain dynamics in monolayer protected metal cluster systems of gold have been studied by the quasielastic neutron scattering technique. Measurements have been carried out with 6, 12, and 18 carbon-long thiolate protected gold clusters of 4 nm core diameter. Dynamics of the monolayers in these systems, as indicated by the quasielastic broadening, were found to evolve continuously with increase in temperature from 270 to 400 K. Analysis of the elastic incoherent structure factor showed that while only a small portion of each chain is dynamically active at low temperature, the dynamics extend to almost the whole chain at 400 K. Although an improved model compared to our earlier reports, involving precessional motion of the chains on a cone is found to explain the observed data, a further improvement with reorientation of the chain around its axis with additional body axis fluctuation was most consistent with the experiment. The studies revealed the existence of complex dynamical motions of alkyl chains on the clusters. The studies suggest that repeated washings provide more space for the monolayer chains as a result of the removal of the phase transfer catalysts between the alkyl chains on the cluster surface. This provides space for greater orientational freedom, resulting in the observed dynamics even at lower temperatures.

PACS number(s): 61.46.Df, 25.40.Fq, 83.10.Mj

INTRODUCTION

Monolayer protected clusters (MPCs) are nanoparticles with monolayer covers.[1] Each MPC has a compact, crystalline metal core of $1-4$ nm diameter which is encapsulated within a shell of tightly packed hydrocarbon chains linked to the core via an atom with specific chemical affinity to the metal. Monolayers of thiols on noble metal surfaces (planar or 2D SAMs) have been the simplest of systems[2] on which many of the fundamental properties such as friction, lubrication, etc. have been investigated.[3] MPCs are important in technology not only due to the higher number density of the molecules at the nanosurface thereby giving diverse attributes to these materials, but also because they preserve the nanodimension of the cluster in a variety of applications. All the experimental studies[4–9] and molecular dynamics simulations[10,11] point to a picture in which organized alkyl-chain bundles are present on specific planes of the cluster surfaces. These monolayers are alternately referred to as three-dimensional self-assembled monolayers (3D SAMs), to distinguish themselves from their planar counterparts (2D SAMs). Due to interactions between the monolayers and the metal cores of adjacent MPCs, the materials may crystallize to yield particle crystals, called superlattices as they possess double periodicity, one due to the metal core and another due to the organized particle assembly.[12–15] There have been several recent efforts to crystallize such materials by incorporating monolayers which effectively participate in intercluster hydrogen bonding.[16,17] The temperature dependent phase behavior of such systems has been a topic of intense investigations in our group as well as in others.[18–23] Phase behavior and dynamics of molecular thin films is intimately related to their conformational order. Orientational freedom of the alkyl chain assembly is one of the critical issues concerning the structure of the monolayers. Applications of monolayer systems in several areas, utilizing distance specific organization of molecules, depend on the structural and conformational rigidity of the monolayer chain.

The quasielastic neutron scattering (QENS) technique was suitably exploited to elucidate interesting results in recent studies.[24–29] Here we report the dynamics of alkyl chains in isolated gold clusters systems with varying chain lengths, using the QENS technique. We specifically investigate the evolution of dynamics in these systems as a function of temperature across the phase transition. This work follows our previous reports[30–33] utilizing QENS, but at improved resolution, over a larger temperature range and energy transfer window, which gave us new insight. These results, in conjunction with the new models have improved our understanding of the monolayer dynamics. Specifically, much more complex dynamics involving the rotation of the molecular axis over a cone with fluctuations in the chain axis have been found. The results suggest that finer details of molecular motions in nanoclusters may be effectively modeled with the aid of neutron scattering. The studies imply that the monolayer structure is intimately connected to the preparation conditions.

EXPERIMENTAL DETAILS

Preparation and characterization of these nanosystems have been discussed previously.[13] Experiments were carried out using a time-of-flight spectrometer IN5 at ILL, Grenoble, France using an incident wavelength of 5 Å and a Q range of $0.2-2.2$ Å^{-1} with an energy resolution 50 μeV. Measurements were carried out with MPCs protected with several thiol (R-SH) molecules of varying chain length, viz., hexanethiol (HT, C_6H_{13}-SH), dodecanethiol (DDT, $C_{12}H_{25}$-SH),

and octadecanethiol (ODT, $C_{18}H_{37}$-SH) stabilized gold (isolated) clusters. The adsorption on nanocluster surfaces result in the loss of thiol proton, leading to the thiolate (R-S^-) group on the surface. The samples, prepared by the two-phase route, were washed four times to get rid of all the unbound thiols and phase transfer reagent. The experiments were conducted over a temperature range of 200–400 K. The nanoparticles are black powders, yielding dark brown to black solutions in toluene. All the systems studied here have been thoroughly characterized by spectroscopy, microscopy, diffraction, and calorimetry.[18–20] In addition, the presence of phase transfer reagent was analyzed by matrix assisted laser desorption ionization mass spectrometry (MALDI MS) using a Voyager DE PRO mass spectrometer of Applied Biosystems. This uses a 337 nm N_2 laser for ionization. We studied the sample by direct laser desorption without any matrix. For neutron scattering studies powder samples were loaded in flat aluminium cans; a sample thickness of ~0.5 mm was chosen such that multiple scattering effects can be neglected. A cryofurnace available at ILL was used for the experiment.

RESULTS AND DISCUSSION

The section below has to be read in the context of the literature on monolayer protected systems and our own previous reports on their dynamics. For clarity, we will bring in certain aspects of their structure as understood from the previous reports.[4,8,9,21,34–36] The monolayers (-S-R, R being C_6H_{13}, $C_{12}H_{25}$, and $C_{18}H_{37}$) have three distinct regions, (1). the head group which binds to the surface of the cluster core, (2). the monolayer body which interacts with the adjacent chains through van der Waals interactions, and (3). the tail group, the -CH_3 in this case, which protrudes outside. The thiolate binding is strong and desorption of the monolayer chain happens only above 270 °C from the gold surface. A majority of the alkyl chains are in all-trans conformation and the chains exhibit solid-like assembly till the phase transition temperature, which vary depending on the chain length.[19] This transition is sharp only in the case of longer chains thiols such as DDT and ODT. In the case of the ODT chain, even the terminal -CH_3 is frozen at room temperature as the methyl r_+ and r_- modes appear in the IR spectrum.[4] At the phase transition temperature, the spectrum resembles that of a liquid, with complete loss of the progression bands. At this point, more gauche defects appear in the spectrum. A schematic of a cluster with its monolayer chains is shown in Fig. 1. Note that a few of the chains can have conformational defects. It is also clear from the scheme that adventitious species can be locked in-between the monolayer chains and their presence provides greater restriction for the motions of the monolayers.

In a neutron scattering experiment from a hydrogeneous system, the observed dynamics mainly corresponds to the self-correlation function of the hydrogen atoms. In the present system, no translational motion is expected. In that case the incoherent scattering law $S_{inc}(Q,\omega)$ describing the rotational dynamics can be written as [37,38]

$$S(Q,\omega) = A(Q)\delta(\omega) + [1 - A(Q)]L[\omega,\Gamma(Q)], \quad (1)$$

where $Q(=k-k_0)$ is the wave vector transfer and $\hbar\omega=E-E_0$ is the energy transfer. The first term is the elastic component and other represents the quasielastic component. $L[\omega,\Gamma(Q)]$ is the Lorentzian function having half width at half maximum Γ, which is related to the reciprocal of the time scale of the motion. It is convenient to analyze the data in terms of the elastic incoherent structure factor (EISF), defined as the fraction of elastic intensity in the total spectrum $\left(\frac{I_{el}}{I_{el}+I_{qel}}\right)$, which provides information about the geometry of the molecular motions. As can be seen from Eq. (1), the EISF is nothing but $A(Q)$.

Quasielastic spectra for the Au-cluster systems (HT, DDT, and ODT stabilized) show the presence of broadening over the whole range of temperatures studied (270–400 K). The quasielastic component was found to evolve continuously with increase of temperature, almost the same way in all the systems. Quasielastic spectra at different temperatures and typically for $Q=1.8$ Å^{-1} are presented in Fig. 2 for the Au-HT (Au-C_6H_{13}-S) system.

Measured QENS spectra were separated into elastic and quasielastic parts by least squares fit after convoluting the scattering law [Eq. (1)] with the instrumental resolution function, which was determined from the measurement of a

Scheme 1 Schematic of a monolayer protected cluster system.

FIG. 1. Schematic of a monolayer protected cluster system.
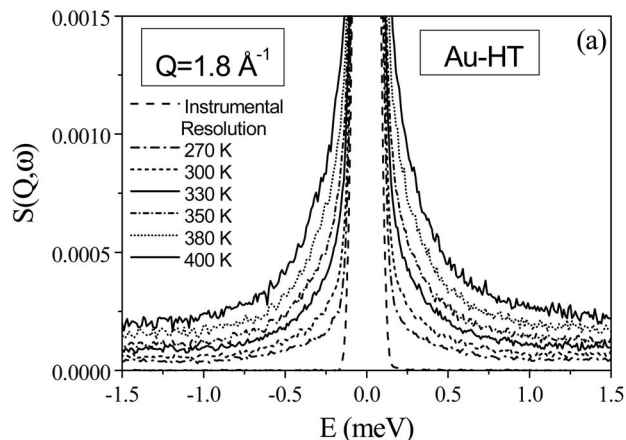
FIG. 2. Typical quasielastic data from Au-HT system at different temperature as obtained using IN5 at ILL, Grenoble at $Q=1.8$ Å^{-1}. Evolution of the quasielastic component with increase in temperature is evident.
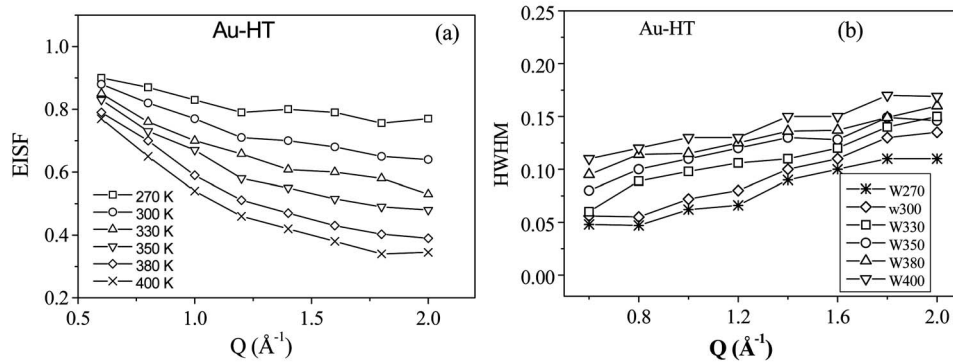
FIG. 3. (a) The extracted EISF and (b) width of the quasielastic part as obtained from the fit with experimental data for Au-HT at different temperatures. The continuous evolution of the alkyl-chain dynamics is evident. Lines are guides to the eye.

vanadium sample having solely elastic scattering. The extracted EISF and width of the quasielastic broadening as obtained from the fit, at different temperatures, are shown in Fig. 3. It is clear from the behavior of the EISF [Fig. 3(a)] that it is strongly temperature dependent and as the temperature is increased, the elastic component decreases while the quasielastic component increases systematically. Variation of the width [Fig. 3(b)] with Q is as expected for a rotational diffusion process and increase of width with temperature suggests a faster motion or increase in diffusion constant, as expected for a thermally activated motion.

Two things can happen with the increase of temperature, (1) higher proportion of the chains can take part in the dynamics and (2) the chains can become more and more flexible. Keeping in mind both possibilities, the generalized scattering law can be written as

$$S(Q,\omega) = (1 - p_x)\delta(\omega) + p_x[A_0\delta(\omega) + (1 - A_0)L(\omega,\Gamma)],$$
(2)

where A_0 is the model EISF and P_x, represents the proportion of mobile or dynamic hydrogen atoms. The total elastic fraction can be written as

$$\text{EISF}_{\text{tot}} = [P_x A_0 + (1 - P_x)].$$
(3)

To extract a functional form for A_0 different dynamical models have to be considered. From the geometry of the MPCs, the simplest model one can envisage is the rotation of the chain about its own axis, namely, uniaxial rotational diffusion (URD, which we will refer to later as model M1) [Fig. 4(a)]. The incoherent scattering law for a particle diffusing on a circle of radius a, with a diffusion coefficient D_r, for a powder sample, are described in Ref. 39.

Considering the molecule as rigid, i.e., side chains are bound to the corelike rods and having uniaxial rotational diffusion around the molecular axis, all the hydrogen atoms will have different radius of rotation and the scattering law should be averaged over the various distances of the hydrogen atoms to the rotation axis. Then the average EISF for a powder sample can be written as

$$A_0 = \overline{A_0(Q)} = \frac{1}{N\pi}\sum_{i=1}^{N}\int_0^{\pi} j_o(2Qa_i \sin x)dx,$$
(4)

where N is the total number of hydrogen atoms in the molecule and a_i is the radius of rotation of ith hydrogen. We

have modeled the alkyl chain as follows. The alkyl chains are assumed to be in an all-trans conformation. The molecular axis is defined as the straight line joining the sulfur atom and the extreme carbon atom as shown in Fig. 4(a). The carbon-carbon distance is taken as 1.537 Å. The carbon-hydrogen distance is taken as 1.11 Å. Angles $\angle$H-C-H and $\angle$C-C-C are assumed to be 107.7°, 111.4°, respectively while the dihedral angle is 180°.

The other possibility could be rotation of the chain axis in a cone (precession model, which we will refer to as model M2). To calculate the EISF for a model where the chain axis is rotating in a cone, let us assume that the long axis of the chain is aligned along the Y axis as shown in Fig. 4(a). Alkyl chains are attached with a sulfur atom in the case of MPCs. The origin is shown to be located on the sulfur atom. Our aim is to calculate the EISF when the chain axis rotates in a cone around the Y-axis. The methodology used here is to calculate the radius of rotation of each hydrogen atom when the chain axis rotates in a cone around the Y axis with an angle θ. Then we calculate the EISFs for each hydrogen according to the uniaxial rotational diffusion model. The final EISF will be calculated after taking the average of the EISFs for all hydrogen atoms in the chain.
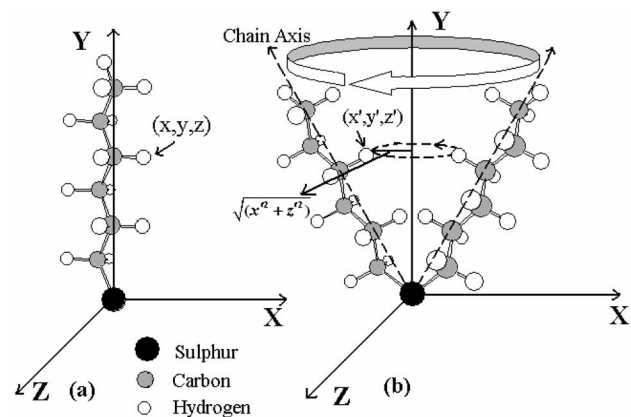
FIG. 4. The structure of the monolayer on the surface of a metal particle. The S atom is on the surface of the particle. (a) Molecular axis of the alkyl chain is oriented along the Y axis and is rotated around it (model M1). (b) Molecular axis is rotated through an angle θ about Z axis (model M2). Molecular axis is shown to undergo a rotation in a cone around the Y axis. Origin is located at the sulfur atom and is assumed to be fixed. $\sqrt{(x'^2 + z'^2)} = r$, is the radius of gyration.
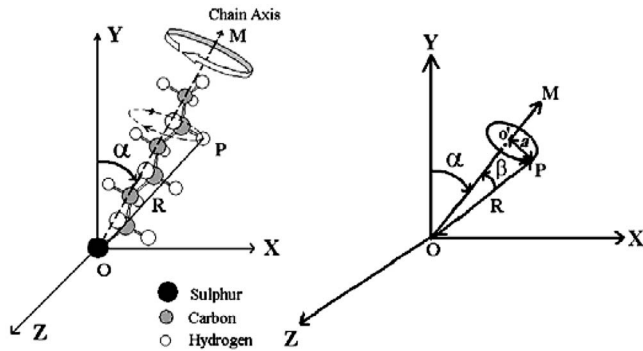
FIG. 5. A hydrogen atom at P is moving with respect to the chain axis (OM). Chain axis, OM fluctuates around the Y axis (model M3).

Let us consider one hydrogen atom whose coordinate is (x,y,z) with respect to the Cartesian coordinate shown in the Fig. 4(a). If we rotate the chain with an angle θ about the z axis, the new coordinate of the same hydrogen atom becomes (x',y',z') [Fig. 4(b)], with the z component remaining the same before and after the rotation. Then the relation between (x,y,z) and (x',y',z') can be written as

$$x' = x\cos\theta + y\sin\theta,$$

$$y' = -x\sin\theta + y\cos\theta,$$

$$z' = z. \qquad (5)$$

The perpendicular distance of the hydrogen atom from the Y axis or the radius of rotation for the hydrogen atom is

$$r = \sqrt{(x'^2 + z'^2)}. \qquad (6)$$

If all the hydrogen atoms are rotating in a circle, each with a different radius of rotation as defined in Eq. (6), then the EISF for uniaxial rotational diffusion for a powder sample can be written as[39]

$$\overline{A_0(Q)} = \frac{1}{N\pi}\sum_{i=1}^{N}\int_0^\pi j_o(2Qr_i\sin x)dx. \qquad (7)$$

N is the total number of hydrogen atoms in a chain and r_i is a function of angle θ. Here the model EISF involves radius of gyration, r_i which is a parameter to be fitted. This r_i basically tells us the angle of rotation (θ) as defined in Eqs. (5) and (6).

Another model, but somewhat similar, is one in which the chain can have rotation about its axis with additional body axis fluctuations. This will be referred to as model M3 and is similar to a "flexible" chain. In order to calculate the EISF for this model, where the chain is rotating about the chain axis (similar to uniaxial rotational diffusion) and the whole chain is fluctuating with some average angle of oscillations, we proceed to consider an alkyl chain that is rotating about its chain axis, OM fixed as shown in Fig. 5 and it simultaneously fluctuates around the Y axis keeping its equilibrium position (namely the sulfur atom) fixed.

Consider a hydrogen, P in the alkyl chain which is moving around an axis, OM on a circle of radius a centered on O' (Fig. 5). If β is the angle between OP and the axis OM, and R the distance of P from origin, the fluctuations of the axis (OM) are described by the following normalized function as described in Ref. 40:

$$f(\alpha) = \frac{\delta}{2\sinh\delta}\exp(\delta\cos\alpha), \qquad (8)$$

where α is the angle between the instantaneous (OM) and mean axis position (OY) and δ is a parameter which characterizes the width of the angular distribution (peaked at $\alpha=0$).

The EISF for rotation about the chain axis and a fluctuation around its equilibrium position can be expressed after averaging over the various distances of the hydrogen atoms from the equilibrium point and their distances from the molecular axis

$$\overline{A_0(Q)} = \frac{1}{N}\sum_{i=1}^{N}\sum_{l=0}^{\infty}(2l+1)j_l^2(Qp_i)S_l^2(\delta)P_l^2(\cos\beta_i) \qquad (9)$$

and

$$\sin\beta_i = \frac{p_i}{q_i}. \qquad (10)$$

Here q_i are the distances of hydrogen atoms in the alkyl chain from the point of fluctuation and p_i are the distances of the same hydrogen atoms from the molecular axis. In Eq. (9), j_l and P_l are the spherical Bessel function and Legendre polynomial of order l, respectively.

Therefore, by knowing the positions of all the hydrogen atoms in the alkyl chain with respect to chain axis, one can fit the experimentally obtained EISF with δ [as defined in Eq. (9)] as parameters. Average amplitudes of fluctuation ($\Delta\alpha$) are then obtained from the fact that $\Delta\alpha=\cos^{-1}(S_l)$. Here, S_l is the orientational order parameter and can be expressed in terms of δ so that $S_l=\langle\cos\alpha\rangle=\coth\delta-\frac{1}{\delta}$.

For the simple uniaxial rotational diffusion, only the proportion of mobile hydrogen, P_x is the parameter to be obtained from the fit. Both models, M2 and M3 have two free parameters to be determined. The proportion of mobile hydrogen P_x is the common parameter for both the models. The other parameter is the precession angle (θ) when the chain moving in a cone (model M2) and the fluctuation amplitude $\Delta\alpha$ for the model where the chain undergoes uniaxial rotation and simultaneous body axis fluctuation (model M3).

The calculated EISFs [Eq. (3)], for different models (A_0) described above, as obtained by least squares fitted to the experimentally extracted EISFs, are shown in Fig. 6. It is apparent from the figure that the description assuming a uniaxial rotational diffusion model [model M1, Eq. (10)], is not good enough. However, it is very evident that with increase of temperature, P_x increases, indicating that an increasing proportion of the chains contribute to the dynamics. As far as the other two models are concerned, it is not very clear which fits the data better for Au-HT system.
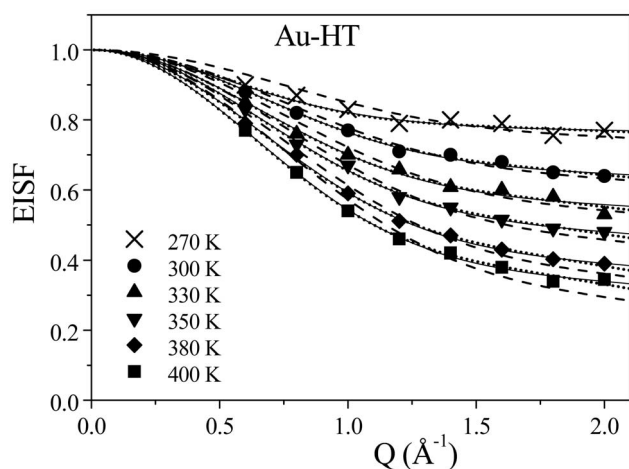
FIG. 6. Experimental EISF, as obtained from QENS data for the Au-HT system, fitted with the (a) uniaxial rotational diffusion mode (M1): dashed line, (b) Chains precessing on a cone (M2): dotted line, and (c) URD with fluctuations of the chain axis (M3): solid line.

The proportion of the dynamical alkyl chain varies from 30 to 90 % in case of the alkyl chain moving in a cone and the precession angle (θ) is of the order of 4°–5°, whereas when the chains perform a uniaxial motion with simultaneous fluctuation of the chains, P_x varies between 25 to 75 % and the average amplitude of oscillation (δ) is about 9°–10° for a change in temperature from 270 to 400 K. By comparing the parameters obtained for the two models, it seems that, while the P_x is higher in case of the chains precessing on a cone model, the amplitude of oscillation is higher for the model with body axis fluctuation; one in some way compensates for the other. Table I gives the parameters obtained at different temperatures for different models. It may be noted that for both the later models [precession (M2) and rotation plus body axis fluctuation (M3)], the hydrogen atoms closer to the core, on the average, move to a lesser extent compared to the outer ones, which is not the case for the simple uniaxial rotational diffusion. In fact the extent of the excursion of the hydrogen atoms increases as it goes away from the core to the end [Figs. 4(b) and 5]. Although it is not possible to select one model over the other for the Au-HT system, later it is shown that model M3 is more physical and consistent for the higher chain length systems.

For the next higher chain length system, Au-DDT the findings are somewhat similar. The simple uniaxial rotational motion is not sufficient to explain the data, however, the description by the model where the chain moves by uniaxial rotational diffusion plus fluctuation is definitely better suited than the one where the chain moves on a cone (data are shown in Fig. 7). The values of P_x vary from 27 to 86 % and δ varies within 5°–10° in the case of model M3 and 30–100 % and 3°–7° for the other model M2 for increase in temperature from 270 to 400 K. Similar to Au-HT, the values of P_x are higher for model M2 and the amplitude of body axis fluctuation within model M3 is more than the cone angle within model M2. Details are given in Table I.

For the highest chain length gold MPC studied, Au-ODT, where the chain contains 18 carbon atoms, the observations

TABLE I. Parameters as obtained from fitting different models to the experimental EISF for Au-MPCs. (Estimated errors on P_x ∼5% and on θ and $\Delta\alpha$ are ∼10%.)

	URD	Precession model		URD+fluctuation	
	P_x (%)	P_x (%)	θ (deg.)	P_x (%)	$\Delta\alpha$ (deg.)
			Au-HT		
270 K	31	32	5	25	10
300 K	46	47	4	40	9
330 K	58	59	4	50	10
350 K	69	69	4	59	9
380 K	81	81	4	69	9
400 K	89	89	5	74	11
			Au-DDT		
270 K	30	30	3	27	5
300 K	51	52	3	46	5
340 K	75	76	4	64	7
380 K	95	94	6	78	8
400 K	100	100	7	86	10
			Au-ODT		
270 K	26	26	0	26	0
300 K	39	40	1	38	1
330 K	65	67	2	59	4
350 K	86	89	3	75	5
380 K	100	104 (100)	4 (5)	84	7
400 K	100	111 (100)	5 (7)	89	8

are very interesting. As with the smaller chain length system, the calculated EISF (Fig. 8) with uniaxial rotational diffusion is not able to account for the experimental data as the temperature is increased. It is interesting to note that at 270 K all three different models lead to the same situation, as the θ and
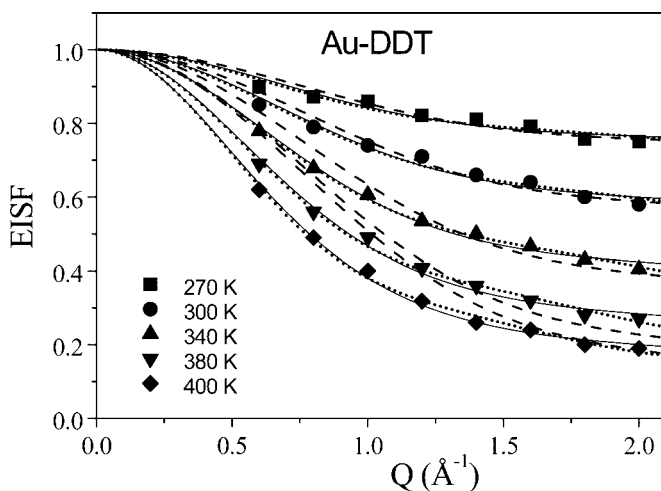
FIG. 7. Experimental EISF, as obtained from QENS data for the Au-DDT system, fitted with (a) model M1: dashed line, (b) model M2: dotted line, and (c) model M3: solid line.
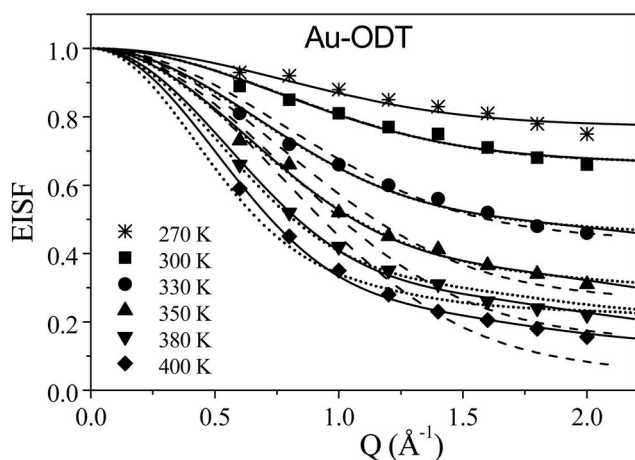
FIG. 8. Experimental EISF, as obtained from QENS data for Au-ODT system, fitted with the (a) model M1: dashed line, (b) model M2: dotted line, and (c) model M3: solid line.

FIG. 9. Variation of the proportion of the Alkyl chain contributing to the dynamics in gold clusters system, as obtained for model M3.

δ of models M2 and M3, respectively turned out to be zero. As temperature is increased, the disorder increases and apart from P_x, the extent of flexibility of the chains reflects in the increase of θ and/or δ. At higher temperatures the calculated EISF models M2 and M3 were almost indistinguishable, but the parameters obtained for model M2, particularly P_x was found to go beyond 100% at 380 K and above, which is not physical. Restricting P_x to 100%, in the fit, resulted in higher θ (parameters shown in parenthesis in the table) than free fitting and the fit was not good at all as shown in Fig. 8. This would suggest that the model where the alkyl chains precess on a cone is not adequate. It may be noted that for the precession model the chains need more space than in the uniaxial rotation plus fluctuation model. As shown in the figure, the model where the alkyl chains undergo simultaneous uniaxial rotational and body axis fluctuation (M3) was able to account for the observed disorder in the data well and the parameters are reasonable and consistent. Within this model, P_x was found to vary between 26 to 89 % with fluctuation, $\Delta\alpha$ ranging from 0° to 8° in the temperature range of 270 to 400 K. Details are given in Table I.

From the foregoing, it can be stated that the model assuming uniaxial rotational diffusion with additional fluctuation of the chain axis (model M3), describes the dynamics of the alkyl chain in isolated cluster systems (gold clusters) at all the temperatures investigated. The variation of P_x as obtained for model M3 is shown in Fig. 9, which clearly shows its monotonic behavior with increase in temperature.

We are aware that the models proposed here are simple, when we consider the various kinds of motions possible for a long alkyl chain. Obviously, conformational changes occurring in the system have to be considered for a fuller understanding. In our earlier temperature dependent infrared spectroscopic investigations,[19] we had shown that the all-trans conformation of the alkyl chains in MPCs undergo systematic changes with increase in temperature and show a melting transition. This is manifested in the C-H stretching modes and the wagging and rocking progression modes. The sudden shift in the methylene stretching modes (d_+ and d_-) to larger
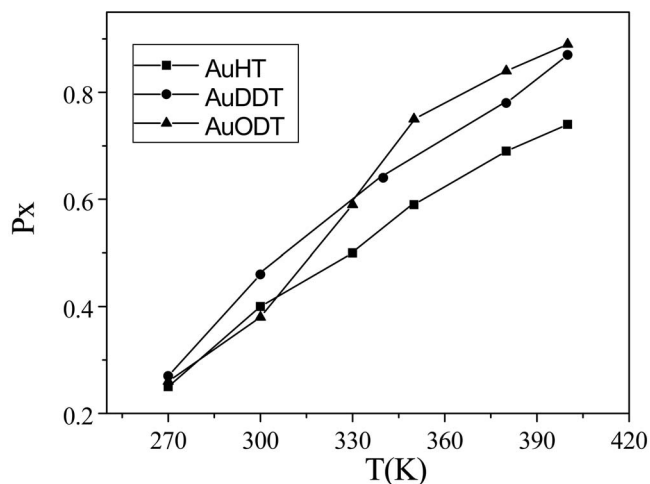
values during phase transition is attributed to the greater number of gauche defects.[41] Occurrence of rotational motion above the alkyl chain phase transition is manifested by the emergence of degeneracy for the methyl group asymmetric stretching modes (r_-). Rotational motion is evident in the methylene δCH_2 mode also. The $(C\text{-}S)_G$ mode retains its intensity throughout the phase transition, while the $(C\text{-}S)_T$ loses its intensity completely indicating that the conformation around the $C\text{-}S$ bond is essentially gauche after the phase transition. These modes do not manifest significant broadening indicating that the bonds closer to the metal surface acquire additional channels of relaxation only at still higher temperatures. The absence of free volume closer to the metal core due to the three dimensionality of the particle inhibits the molecule from behaving like an isolated alkane molecule. Thus, although the system shows a transition similar to crystalline alkanes, with creation of gauche defects, the motions are not identical as in the case of free alkanes as one end of the chain is rigidly held where the molecular packing does not provide adequate space for additional motions. Thus the amplitude of atomic excursions will be smaller which would make motions less complicated in comparison to those in free alkanes.

We had suggested that the rotator state does not exist in AuMPCs in the case of longer chain length monolayers at room temperature.[32] The current data suggests monotonic increase in dynamics as a function of temperature. The presence of rotational dynamics is evident even at the lowest temperature investigated. The reason for this difference appears to be the gradual removal of the phase transfer reagent in repeated washings. It has been shown from previous reports that the monolayer chains contain up to 5% of phase transfer reagent in them[42] and a loss of this impurity happens only slowly, in repeated and longer term washings. The samples used here have been soaked in a large excess of acetone for one week at a time and the precipitation was achieved in this period. This resulted in the slow removal of the phase transfer reagents giving more space to the monolayer chains. To support this conclusion, we present the posi-
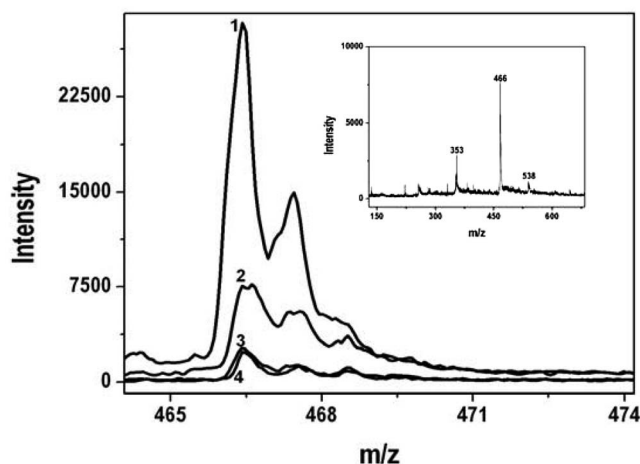
FIG. 10. MALDI MS data of AuC_{18} MPC as a function of repeated washing. Traces from the top to the bottom are after one to four washings. The peak at m/z 466 (actually at 466.4) is due to $(C_8H_{17})_4N^+$. The higher mass number peaks at 1 amu spacing are due to its pattern. The spectrum in a larger mass range after one washing, showing the sulfide peak at m/z 538 is shown in the inset. The peak at m/z 353 is due to $(C_8H_{17})_3N^+$.

tive ion MALDI MS spectra of the MPCs before and after repeated washing (Fig. 10). The mass spectrum shows the presence of the peak at m/z 466 corresponding to $(C_8H_{17})_4N^+$ which reduces in intensity upon repeated washing. Loss of C_8H_{17} is shown up in the spectra as a peak at m/z 353 (loss of 113 due to C_8H_{17} from 466). It may be noted that it is difficult to completely remove this species from the material and MALDI sensitivity for this ion is very high so that even at trace levels it appears in the spectrum. As a result of the increased sensitivity of MALDI towards the phase transfer reagent, the $C_{18}H_{37}$-S-$C_{18}H_{37}$ (m/z 538), due to desorption of the monolayer chain, appears as a weak peak. Removal of the traces of phase transfer reagent pro-

vided the space required for the thiolate chains to exhibit dynamical motions.

CONCLUSIONS

A detailed description of alkyl chain reorientations was presented for monolayer protected isolated gold cluster system on the basis of high-resolution neutron scattering studies. It is found that the dynamics of alkyl chains evolve continuously with temperature. At low temperatures, only the chain termini take part in the dynamics and not all the hydrogens are participating in the reorientations. As the temperature increases, more and more hydrogens contribute to the dynamics. It is also established that reorientation motions of alkyl chains are not following simple uniaxial rotational diffusion around the chain axis. More complex motions such as reorientations of alkyl chains in a cone or uniaxial rotational diffusion of chains around the axis with additional body axis fluctuations are involved, which explain the experimentally obtained EISF well. It is found that the uniaxial rotation plus body axis fluctuation is the most suitable model to describe the QENS data consistently, which is expected intuitively. The precession model requires larger space which is probably not available due to the way the chains are organized on the metal cluster surface. The fraction of hydrogens taking part in the dynamics increases with temperature for all the systems with different alkyl-chain lengths. Repeated washings of the sample provide more space for the monolayer chains as a result of the removal of the phase transfer catalysts interlocking the alkyl chains on the cluster surface. This makes room for greater orientational freedom, explaining the observed dynamics even at lower temperatures.

*Email address: mukhop@barc.ernet.in

†Email address: pradeep@iitm.ac.in

[1] A. C. Templeton, W. P. Wuelfing, and R. W. Murray, Acc. Chem. Res. **33**, 27 (2000).

[2] G. E. Poirier, Chem. Rev. (Washington, D.C.) **97**, 1117 (1997).

[3] R. W. Carpick and M. Salmeron, Chem. Rev. (Washington, D.C.) **97**, 1163 (1997).

[4] M. J. Hostetler, J. J. Stokes, and R. W. Murray, Langmuir **12**, 3604 (1996).

[5] R. H. Terril, T. A. Postlethwaite, C. H. Chen, C. D. Poon, A. Terzis, A. Chen, J. E. Hutchison, M. R. Clark, G. Wignall, J. D. Londono, R. Superfine, M. Falvo, C. S. Johnson Jr., E. T. Samulski, and R. W. Murray, J. Am. Chem. Soc. **117**, 12537 (1995).

[6] F. Bensebaa, T. H. Ellis, A. Badia, and R. B. Lennox, J. Vac. Sci. Technol. A **13**, 1331 (1995).

[7] F. Bensebaa, T. H. Ellis, A. Badia, and R. B. Lennox, Langmuir **14**, 2361 (1998).

[8] A. Badia, S. Singh, L. Demers, L. Cuccia, G. R. Brown, and R. B. Lennox, Chem.-Eur. J. **2**, 359 (1996).

[9] A. Badia, L. Cuccia, L. Demers, F. E. Morin, and R. B. Lennox, J. Am. Chem. Soc. **119**, 2682 (1997).

[10] W. D. Luedtke and U. Landman, J. Phys. Chem. **100**, 13323 (1996).

[11] W. D. Luedtke and U. Landman, J. Phys. Chem. B **102**, 6566 (1998).

[12] K. V. Sarathy, G. U. Kulkarni, and C. N. R. Rao, J. Chem. Soc., Chem. Commun. 537 (1997).

[13] N. K. Chaki and K. P. Vijayamohanan, J. Phys. Chem. B **109**, 2552 (2005).

[14] Z. L. Wang, S. A. Harfenist, R. L. Whetten, J. Bentley, and N. D. Evans, J. Phys. Chem. B **102**, 3068 (1998).

[15] B. L. V. Prasad, S. I. Stoeva, C. M. Sorensen, and K. J. Klabunde, Chem. Mater. **15**, 935 (2003).

[16] S. Wang, H. Yao, S. Sato, and K. Kimura, J. Am. Chem. Soc.

126, 7438 (2004).

[17] H. Yao, T. Minami, A. Hori, M. Koma, and K. Kimura, J. Phys. Chem. B **110**, 14040 (2006).

[18] N. Sandhyarani, T. Pradeep, J. Chakrabarti, M. Yousuf, and H. K. Sahu, Phys. Rev. B **62**, R739 (2000).

[19] N. Sandhyarani, M. P. Antony, G. P. Selvam, and T. Pradeep, J. Chem. Phys. **113**, 9794 (2000).

[20] N. Sandhyarani, M. R. Resmi, R. Unnikrishnan, K. Vidyasagar, S. Ma, M. P. Antony, G. P. Selvam, V. Visalakshi, N. Chandrakumar, K. Pandian, Y. T. Tao, and T. Pradeep, Chem. Mater. **12**, 104 (2000).

[21] L. H. Dubois and R. G. Nuzzo, Annu. Rev. Phys. Chem. **43**, 437 (1992).

[22] B. A. Korgel and D. Fitzmaurice, Phys. Rev. B **59**, 14191 (1999).

[23] J. R. Heath, C. M. Knobler, and D. V. Leff, J. Phys. Chem. B **101**, 189 (1997).

[24] F. Y. Hansen, L. Criswell, D. Fuhrmann, K. W. Herwig, A. Diama, R. M. Dimeo, D. A. Neumann, U. G. Volkmann, and H. Taub, Phys. Rev. Lett. **92**, 46103 (2004).

[25] K. W. Herwig, D. Fuhrmann, L. Criswell, H. Taub, Y. Hansen, R. Dimeo, and D. A. Neumann, J. Phys. IV **10**, 157 (2000).

[26] K. H. Herwig, Z. Wu, P. H. Dai, Taub, and F. Y. Hansen, J. Chem. Phys. **107**, 5186 (1997).

[27] M. A. Castro, S. M. Clarke, A. Inaba, C. C. Dong, and R. K. Thomas, J. Phys. Chem. B **102**, 777 (1998).

[28] M. A. Castro, S. M. Clarke, A. Inaba, T. Arnold, and R. K. Thomas, J. Phys. Chem. Solids **60**, 1495 (1999).

[29] J. M. Gay, P. Stocker, D. Degenhardt, and H. Lauter, Phys. Rev. B **46**, 1195 (1992).

[30] T. Pradeep, S. Mitra, A. S. Nair, and R. Mukhopadhyay, J. Phys. Chem. B **108**, 7012 (2004).

[31] R. Mukhopadhyay, S. Mitra, I. Tsukushi, S. Ikeda, and T. Pradeep, Chem. Phys. **292**, 223 (2003).

[32] R. Mukhopadhyay, S. Mitra, I. Tsukushi, S. Ikeda, and T. Pradeep, J. Chem. Phys. **118**, 4614 (2003).

[33] S. Mitra, B. Nair, T. Pradeep, P. S. Goyal, and R. Mukhopadhyay, J. Phys. Chem. B **106**, 3960 (2002).

[34] N. Sandhyarani and T. Pradeep. Int. Rev. Phys. Chem. **22**, 221 (2003).

[35] N. Sandhyarani and T. Pradeep, Pure Appl. Chem. **74**, 1593 (2002).

[36] A. C. Templton, M. J. Hostetler, E. K. Warmoth, S. Chen, C. M. Hartshorn, V. M. Krishnamurthy, M. D. E. Forbes, and R. W. Murray, J. Am. Chem. Soc. **120**, 4845 (1998).

[37] M. Bee, *Quasielastic Neutron Scattering* (Adam-Hilger, Bristol, 1988).

[38] W. Press, *Single Particle Rotations in Molecular Crystals* (Springer, Berlin, 1981).

[39] A. J. Dianoux, F. Volino, and H. Hervet, Mol. Phys. **30**, 1181 (1975).

[40] F. Volino, A. J. Dianoux, and H. Hervet, J. Phys. Colloq. **37**, C3–55 (1976).

[41] M. A. MacPhail, H. L. Strauss, R. G. Snyder, and C. A. Elliger, J. Phys. Chem. **88**, 334 (1982); M. Maroncelli, S. P. Qi, H. L. Strauss, and R. G. Snyder, J. Am. Chem. Soc. **104**, 6237 (1982); R. G. Snyder, H. L. Strauss, and C. A. Elliger, J. Phys. Chem. **86**, 5145 (1982).

[42] C. A. Waters, A. J. Mills, K. A. Johnson, and D. Schiffrin, J. Chem. Soc., Chem. Commun. 540 (2003).